agronomy

MDPI

*Article*

# Carbon Budget of Paddy Fields after Implementing Water-Saving Irrigation in Northeast China

**Tiecheng Li [1,2], Tangzhe Nie [3], Peng Chen [4], Zuohe Zhang [1,2,5], Jiaxin Lan [1], Zhongxue Zhang [1,2,*], Zhijuan Qi [1,2,*], Yu Han [1,2] and Lili Jiang [1,2]**

1 School of Water Conservancy and Civil Engineering, Northeast Agricultural University, Harbin 150030, China; b210101005@neau.edu.cn (T.L.); zhangzuohe@126.com (Z.Z.); lanjiaxin96@163.com (J.L.); 15904505762@163.com (Y.H.); jianglili94@163.com (L.J.)
2 Key Laboratory of Agricultural Water Resources Use, Ministry of Agriculture and Rural Affairs, Northeast Agricultural University, Harbin 150030, China
3 School of Water Conservancy and Electric Power, Heilongjiang University, Harbin 150006, China; 2019036@hlju.edu.cn
4 College of Agricultural Science and Engineering, Hohai University, Nanjing 210024, China; chenpeng_isotope@163.com
5 School of Agriculture and Hydraulic Engineering, Suihua University, Suihua 152001, China
* Correspondence: zhangzhongxue@neau.edu.cn (Z.Z.); zhijuan.qi@neau.edu.cn (Z.Q.)

**Abstract:** Water-saving irrigation is recognized as an effective agricultural management due to water security and environmental protection problems. In Northeast China, an increasing number of paddy fields are shifting from conventional irrigation to water-saving irrigation. However, there is limited knowledge regarding the carbon (C) budget of paddy fields after implementing water-saving irrigation in Northeast China. A 2-year consecutive field study was performed from 2018 to 2019 using three different irrigation regimes (conventional irrigation (FI), controlled irrigation (CI), and intermittent irrigation (II)) and two nitrogen (N) fertilization levels (110 and 165 kg N ha$^{-1}$) in a paddy field of Northeast China. The present study aimed to quantify the net ecosystem C budget (*NECB*) and net global warming potential (*net GWP*) after the implementation of water-saving irrigation in Northeast China. Both CI and II enhanced the C sequestration capacity of this paddy field. The net primary productivity (*NPP*) under CI and II was higher than FI by 18–38% and 11–33%, respectively, when the same N fertilization level was applied. The *NECB* ranged from 1151 to 2663 kg C ha$^{-1}$, indicating that all treatments acted as net C sinks. II increased the *NECB* through increasing *NPP*, which exceeded increased removal of harvest and C mineralized losses. Under II, the *NECB* was significantly higher than FI and CI when the same N fertilization level was applied ($p < 0.05$). The *net GWP* under II and CI was significantly lower than FI ($p < 0.05$). The *net GWP* under II was lower than CI when the N fertilization level was 165 kg N ha$^{-1}$, but no significant differences were detected. These results demonstrated that the II with 165 kg N ha$^{-1}$ of paddy fields strongly decreased *net GWP* in Northeast China to combat global climate change.

**Keywords:** water-saving irrigation; net ecosystem carbon budget; net primary production; carbon mineralized losses; net global warming potential



**Citation:** Li, T.; Nie, T.; Chen, P.; Zhang, Z.; Lan, J.; Zhang, Z.; Qi, Z.; Han, Y.; Jiang, L. Carbon Budget of Paddy Fields after Implementing Water-Saving Irrigation in Northeast China. *Agronomy* **2022**, *12*, 1481. https://doi.org/10.3390/agronomy12061481

Academic Editor: José L.S. Pereira

Received: 8 May 2022
Accepted: 17 June 2022
Published: 20 June 2022



## 1. Introduction

Rice is a main food for >50% of the world's population. As the largest rice-producing country, China shares ~19% of the rice-growing area and 32% of the rice yield in the world [1]. Given the decline in the availability of water resources and increasing demands and environmental benefits for water-saving irrigation, several paddy fields with conventional irrigation (FI) have been replaced by water-saving irrigation in China [2,3]. Some widely used water-saving irrigation regimes, including rain-gathering irrigation (RGI), controlled irrigation (CI), and intermittent irrigation (II), have been applied across China,

of which CI and II are the main regimes in Northern China [4–6]. Previous studies demonstrated that water-saving irrigation regimes enhance C sequestration by affecting plant growth due to differences in the amount of irrigation, irrigation frequency, and irrigation intervals during the rice cropping season [7,8]. Akter et al. reported that appropriate water-saving irrigation regimes promoted root activity, which thereby benefited other physiological processes and resulted in rice growth [9]. Wang et al. found that the application of water-saving irrigation reduced N loss, and more N was absorbed for rice growth, which thereby increased crop yields [10]. Moreover, some studies have reported that water-saving irrigation will affect plant growth and greenhouse gas (GHG) emissions after its implementation [11–13].

The effects of irrigation on GHG emissions are a result of soil moisture regulation. It is well-known that soil moisture is a key factor in GHG emission regulation as it affects microbe activities and other relevant processes [14,15]. Water-saving irrigation improves soil aeration by regulating soil moisture. Soil aerobic conditions strengthen microbial activities and soil respiration and thus promote $CO_2$ production, which is emitted from the soil through the roots and soil respiration [16]. Qi et al. reported that the irrigation mode, irrigation volume, and irrigation frequency influence $CO_2$ emissions [17]. Yang et al. reported that CI strongly increased soil respiration, which resulted in a decrease in NEE in paddy fields [18]. Nevertheless, soil aerobic conditions significantly inhibit $CH_4$ emissions as they impede methanogen activities and all related processes and increase the redox potential [19]. The results of two experiments indicated that CI decreased $CH_4$ emissions by 34% and 83.5%, respectively, compared to FI in Northeast and Southeast China [20,21]. Previous studies investigated GHG emissions and C sequestration under different water-saving irrigation regimes. However, the C budget of paddy field ecosystems remains uncertain after water-saving irrigation is implemented. Paddy field ecosystems may act as either a C sink or C source after water-saving irrigation is implemented. Therefore, it is important to understand the balance between C sequestration and GHG emissions in paddy fields, as well as enhance the C sequestration capacity to establish water-saving agricultural production.

Aiming to meet the needs of rice yields in China, rice-growing areas have increased rapidly in Northeast China, especially in Heilongjiang Province [22]. The National Bureau of Statistics of China reported that the total paddy field area was $2.68 \times 10^6$ ha in 2000 and increased at a rate of $0.16 \times 10^6$ ha year$^{-1}$. In 2017, the total paddy field area of Northeast China reached $5.62 \times 10^6$ ha. Currently, FI is used in most areas of Northeast China. Such a rapid increase in paddy field areas requires a great deal of water for agricultural irrigation. Moreover, the population growth, urbanization, and industrialization of Northeast China, along with water resource quality decline, have aggravated the dire shortage of agricultural irrigation water. Due to the severe shortage of agricultural irrigation water, government departments have attempted to promote water-saving irrigation through training and other means every year. In 2018, the rice water-saving irrigation area of Heilongjiang Province reached $1.24 \times 10^6$ ha, and the annual water savings was $1.85 \times 10^8$ m$^3$ [23]. Additionally, the effects of environmental factors and basic soil physical-chemical properties on rice growth and C mineralized losses vary across different regions. Therefore, selecting the most appropriate irrigation regime is vitally important for Northeast China.

This study aimed to address the following questions: (1) Which irrigation regimes are best for Northeast China? (2) How much of an effect does water-saving irrigation have on the balance between C mineralized losses and C sequestration? We aimed to quantify the net ecosystem C budget (*NECB*) and the emissions of $CH_4$, as well as their contributions to the *net GWP* after implementing water-saving irrigation. The aims of this study were to (1) explore whether paddy fields act as a C sink or C source after implementing water-saving irrigation, and (2) identify which water-saving irrigation regime can decrease *net GWP* in Northeast China to combat global climate change.

## 2. Materials and Methods

### *2.1. Site Description*

The field site was located in Suihua, Heilongjiang Province, China (46°57′28″ N, 127°40′45″ E; 168 m.a.s.l.), which is a typical black soil paddy field growing area at the intersection of the Songnen Plain and Xiao Xing'an Mountains. The site has a monsoon climate in a cold temperate zone. In this region, the average annual precipitation was 577 mm, and the average air temperature was 1.69 °C. The soil texture of this region was classified as sandy clay, and the physical-chemical properties of the 0–20 cm layer were pH 6.6 ($H_2O$, 1:1), 40.6 g $kg^{-1}$ organic matter, 186.8 mg $kg^{-1}$ alkaline N, 34.9 mg $kg^{-1}$ available *p*, and 106.8 mg $kg^{-1}$ available K.

The dominant cropping system in the region is single cropping rice, which is cultivated ~120 days during the summer and autumn. Thereafter, the soil is frozen under extremely cold conditions during the fallow season. Prior to experimentation, the test field had rice planted for >20 years and received frequent farmyard manure input. Measurements were carried out in a 2-year field experiment from 2018 to 2019. Straw was shredded (<5 cm) by an automated pulverizer and returned to the soil at a depth of 20 cm at the time of harvest.

### *2.2. Experimental Design*

The experiment was laid out in a spilt-plot design with a water-saving irrigation regime, and N fertilization was used as sub-plots. The irrigation regimes included (1) FI, (2) CI, and (3) II (Table 1). II sets the irrigation amount and intervals during the rice cropping season to make the paddy field in shallow water or no surface water conditions. CI keeps the paddy field in shallow water only in the turning green stage while allowing the paddy field under no surface water conditions throughout the rest of the cropping season. In the experimental area, the amount of N, $P_2O_5$, and $K_2O$ is recommended as 110, 45, and 80 kg $ha^{-1}$, respectively [24–27]. The N fertilization levels consisted of (1) 110 kg N $ha^{-1}$ (N110) and (2) 165 kg N $ha^{-1}$ (N165) (>50% conventional N fertilization application; more N fertilizer is applied after returning straw) [28,29]. One day before rice transplanting, 45% of the N fertilizer was applied as basal fertilizer. Twenty-four and seventy-two days after transplanting, 20% and 35% of N fertilizer were applied as tillering and grain fertilizer, respectively. The application rates of $P_2O_5$ and $K_2O$ were the same in all treatments (45 kg $ha^{-1}$ $P_2O_5$ and 80 kg $ha^{-1}$ $K_2O$). Before rice transplanting, 50% of the $K_2O$ was applied, and the other 50% of the $K_2O$ was applied at the leaf age of 8.5. Each treatment was laid out with 3 replicates. In total, there were 6 main-plots and 18 sub-plots. The size of the sub-plots was 10 × 10 m. Between each plot, a concrete barrier (height: 40 cm) was laid down as a barrier to prevent the exchange of water and fertilizer. Twenty-one-day-old rice seedlings (3 plants per hill, Longqing 3, China) were transplanted by automatic machine. The planting density was 16.67 cm × 30 cm. All other agricultural management practices, including raising seeding, pesticide application, and harvesting, were the same for each treatment [30]. In 2018 and 2019, the seedlings were transplanted on May 18 and May 19 and rice was harvested on September 22 and September 21.

**Table 1.** Different water management regime at rice growth stages.

| Irrigation Regime | Turning -Green Stage | Early Tillering Stage | Middle Tillering Stage | Late Tillering Stage | Jointing -Booting Stage | Heading-Flowering Stage | Milk Stage | Yellow -Ripe Stage |
|---|---|---|---|---|---|---|---|---|
| FI | 0~30 mm | 0~50 mm | 0~50 mm | Drainage | 0~50 mm | 0~50 mm | 0~50 mm | Naturally drying |
| CI | 0~30 mm | 0.7 θs~0 | 0.7 θs~0 | Drainage | 0.8 θs~0 | 0.8 θs~0 | 0.7 θs~0 | Naturally drying |
| II | 0~30 mm | 0~40 mm | 0~40 mm | Drainage | 0~30 mm | 0~40 mm | 0~40 mm | Naturally drying |

Note: θs refers to soil saturated water content mass fraction in the root layer. FI, conventional irrigation; CI, controlled irrigation; II, intermittent irrigation.

### 2.3. C Mineralized Losses

Heterotrophic respiration (*Rh*) was measured in situ using LI-COR closed-chamber soil respiration system (LI-COR 8100; Li-cor Inc; Lincoln, MI, USA) [31]. PVC collars (10 cm inner diameter, 50 cm in height) were laid out with 3 replicates in each plot during the rice cropping season. In each collar, rice was not cultivated, and weeds were entirely removed. PVC collars were drilled to 5–50 cm, through which the management of water and fertilizer inside and outside the PVC collars were consistent, and roots were prevented from entering. PVC collars were inserted into the soil to 45 cm after rice was transplanted. Measurements were carried out from transplantation to harvest once per week. The measuring time was fixed between 9:00 and 11:00 a.m., as the *Rh* and $CH_4$ fluxes during this time quantum were close to the mean daily *Rh* and $CH_4$ fluxes [32]. In the event of heavy rainfall, the measurement time was delayed. Methane fluxes were measured at the same time on the same day using the static chamber-gas chromatography method. Static chambers were also laid out with 3 replicates in each plot during the rice cropping season. The static chambers consisted of a chamber and stainless-steel base. The chambers were made of transparent organic glass. Each chamber was equipped with an air thermometer and electronic fan. Chambers were removed from the base, except during gas collection. The stainless-steel base was embedded in each plot before transplanting with a sealing groove (3 cm width, 5 cm height) reserved at the top. While taking measurements, water was injected to seal the groove to avoid gas exchange in the chamber with outside air. At 0, 10, 20, and 30 min after chamber closure, 4 gas samples were collected using a 50 mL E-Switch gas bag via a rubber tube for each $CH_4$ flux measurement. The temperature inside the chamber was also recorded [33]. All gas samples were analyzed within 24 h using gas chromatography (GC-2010 Plus; Shimadzu Corporation; Kyoto; Japan). The gas chromatograph was equipped with a flame ionization detector (FID); methane concentration was analyzed at 200 °C; the carrier gas was $N_2$ with a purity of 99.99%.

Methane fluxes were calculated based on changes in their concentrations throughout the sampling period and estimated as the slope of the curve of the concentration versus time [34]. Then, $CH_4$ fluxes were calculated as follows [35]:

$$F = \rho \times h \times dc/dt \times 273/273 + T \quad (1)$$

where $F$ is the $CH_4$ fluxes (mg $m^{-2}$ $h^{-1}$), $\rho$ is the density of $CH_4$ under a standardized state (0.714 mg $cm^{-3}$), $h$ is the effective height of the chamber above the soil or surface water (m), $dc/dt$ is the rate of increase of $CH_4$ gas concentrations in the chamber (g $m^{-3}$ $d^{-1}$), and $T$ is the mean air temperature inside the chamber at the time of sampling.

The *seasonal Rh* (kg C $ha^{-1}$) and $CH_4$ fluxes (kg C $ha^{-1}$) for the entire cropping period were calculated as follows [36]:

$$Seasonal\ Rh\ and\ CH_4 = \sum_{i}^{n} (E_i \times D_i) \quad (2)$$

where $E_i$ is the *Rh* (μmol $m^{-2}$ $s^{-1}$) and $CH_4$ fluxes (mg $m^{-2}$ $h^{-1}$) at the $i$th interval during sampling, $D_i$ is the number of days between $i$th sampling and $(i-1)$th sampling, and $n$ is the sampling number.

### 2.4. NECB Calculation

Based on a mass C budget approach, the *NECB* (kg C $ha^{-1}$) was calculated between the rate of C gain or loss in a cropping system. Previous studies demonstrated that the *NECB* with a positive value indicates that paddy fields act as a C sink, and a negative value indicates a C source. The *NECB* was calculated as follows [37,38].

$$Re = Ra + Rh \quad (3)$$

$$NECB = \sum Cinput - \sum Coutput - (NPP + Ra) - (Re + Harvest + CH_4) = NPP - Rh - Harvest - CH_4 \quad (4)$$

where *NPP* (kg C $ha^{-1}$) is the net primary production during rice cropping season and the fallow season [39], and *Re* is the sum of plant respiration *Ra* and *Rh* [40]; *Rh* was measured using the above closed-chamber soil respiration system, and $CH_4$ fluxes were measured by the static chamber-gas chromatography method. In the event that all residues were returned to the field, only grain was moved from the field at the time of harvest. Soil C losses through runoff and leaching were typically excluded from the calculations and therefore not included in the current study.

Grain, stem, and leaf were harvested using sickle in each plot, and the size of the sampling frame was 100 × 100 cm. Roots were acquired from the 30 cm soil layer using a root extractor (5.8 cm inner diameter) in each plot and were washed using a pressure-water gun [41]. Grain, stem, leaf, and root were placed in a drying oven at 105 °C for 30 min, dried at 70 °C to a constant mass, and weighed. Grain, stem, leaf, and root were ground into a powder. Then, sample C was measured using a vario TOC elemental analyzer (Elementar vario TOC; Elementar; Hanau; Germany). The *NPP* of rice during rice cropping was calculated as follows [42–45]:

$$NPP = NPP_{grain} + NPP_{stem} + NPP_{leaf} + NPP_{root} + NPP_{litter} + NPP_{rhizodeposit} \quad (5)$$

in which rice $NPP_{(grain,\ stem,\ leaf,\ root)}$ was calculated using the dried matter weight multiplied by the C content at the time of harvest. $NPP_{litter}$ and $NPP_{rhizodepoait}$ were estimated by other rules. Litter accounted for ~5% of the total dried matter weight, and the C leaf content was used to calculate $NPP_{litter}$ [46]. $NPP_{rhizodepoait}$ mainly included exudates, exfoliated root hairs, and dead root and was calculated as 11% of the total C content [47].

### 2.5. Net Global Warming Potential

The *net GWP* (kg C $ha^{-1}$) was used to estimate the climatic impact of the paddy field system after implementing water-saving irrigation. $N_2O$ emissions were not considered in this study. The *net GWP* was calculated as follows [48]:

$$Net\ GWP = 28 \times Seasonal\ C\ H_4 - 44/12 \times NECB \quad (6)$$

where the warming potential of $CH_4$ was 28 on a 100-year time horizon [49], *Seasonal* $CH_4$ represents cumulative fluxes of $CH_4$ during the entire cropping period, and *NECB* represents the rate of C gain or C loss in a cropping system; 44/12 was the conversion coefficient of C to $CO_2$.

### 2.6. Statistical Analysis

All formula calculations were calculated using Excel 2010. Statistical analyses were performed by SPSS v19.0 (IBM). Univariate multivariate analysis of variance was used to test the effects of irrigation regime, N fertilization, year, and their interactions on *NPP* and the components of *NECB* and *net GWP*. Three-way ANOVAs were used to evaluate significant differences in all treatments. The significant threshold of all statistical analyses was $p < 0.05$. All figures were visualized using ORIGIN v9.0 (OriginLab).

## 3. Results

### 3.1. Environmental Conditions

The typical climatic conditions of the study site were observed during the 2-year field study; environmental conditions did not differ considerably from 2018 to 2019 (Figure 1). During rice cultivation, the daily air temperature ranged from 2.0 °C to 37.6 °C in 2018 and from 1.7 °C to 33.7 °C in 2019. The seasonal precipitation in 2018 (563.6 mm) was higher during rice cultivation than in 2019 (542.5 mm).

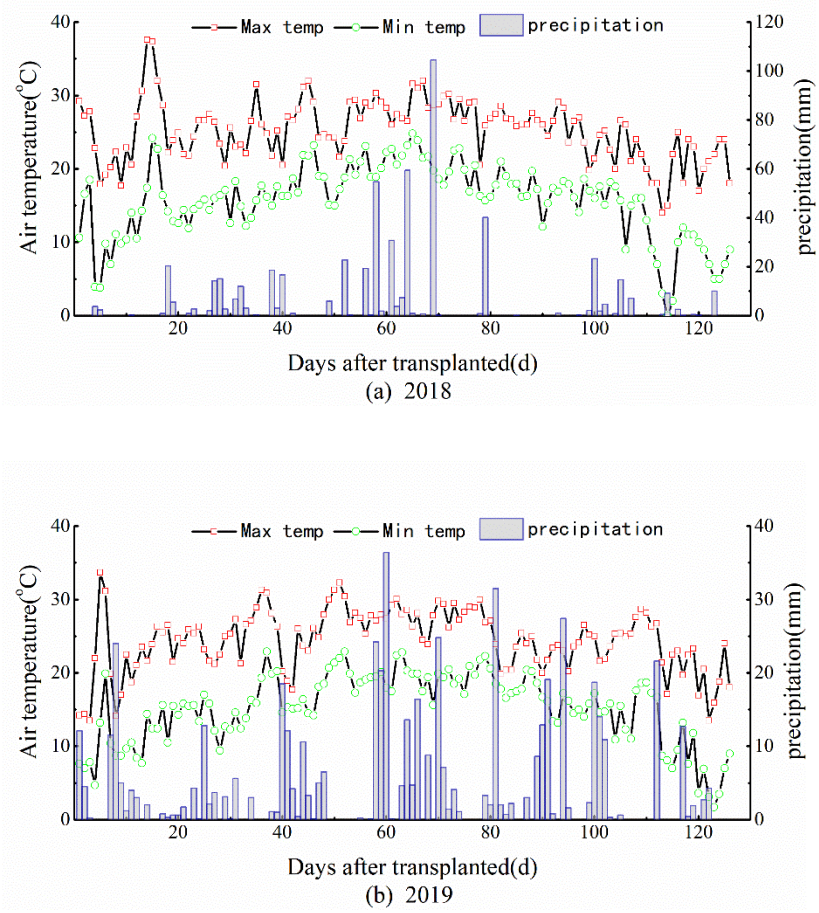


**Figure 1.** Changes in maximum and minimum air temperature and precipitation in (**a**) 2018 and (**b**) 2019.

### *3.2. Net Primary Productivity*

The rice dried matter weight and their C contents are presented in Figure 2. Compared with FI, CI and II increased dried matter weight and rice C contents when the same N fertilization application level was applied. The increased intensity of rice dried matter weight of CI was strongest, and CI and II were higher than FI by 15–32% and 9–30%, respectively. The C contents of each part of the rice plant did not significantly differ among the three irrigation regimes. The dried matter weight and C contents of rice under N165 were higher than N110.

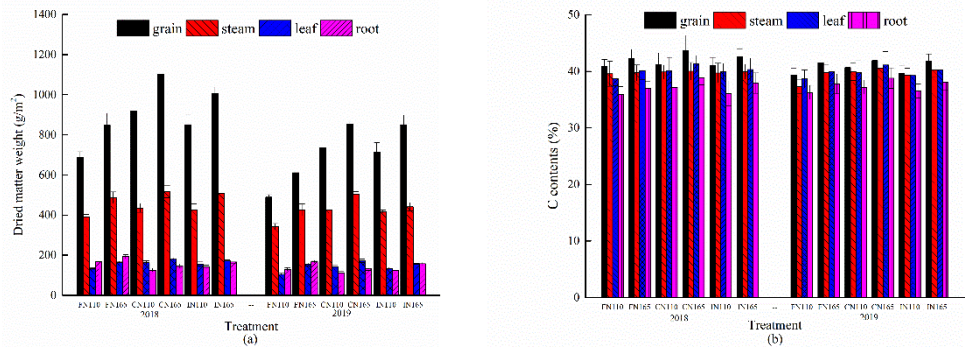


**Figure 2.** Changes of (**a**) dried matter weight and (**b**) their C contents in paddy fields after the implementation of water-saving irrigation.

The *NPP* components are summarized in Table 2. $NPP_{grain}$, $NPP_{stem}$, $NPP_{leaf}$, $NPP_{litter}$, $NPP_{rhizodeposit}$, and *NPP* under CI and II were significantly higher than FI when the same N fertilization level was applied ($p < 0.05$). Additionally, $NPP_{grain}$, $NPP_{stem}$, $NPP_{leaf}$, $NPP_{litter}$, $NPP_{rhizodeposit}$, and *NPP* under CI were higher than II. *NPP* under CI and II were higher than FI by 18–38% and 11–33%, respectively. However, $NPP_{root}$ under FI was higher than CI and II. $NPP_{grain}$, $NPP_{stem}$, $NPP_{leaf}$, $NPP_{root}$, $NPP_{litter}$, $NPP_{rhizodeposit}$, and *NPP* under N165 were all significantly higher than N110. These changes exhibited similar trends in 2018 and 2019. Nonetheless, $NPP_{grain}$, $NPP_{stem}$, $NPP_{leaf}$, $NPP_{litter}$, $NPP_{rhizodeposit}$, and *NPP* of each treatment in 2018 were higher than in 2019.

**Table 2.** Changes in *NPP* components in paddy fields after the implementation of water-saving irrigation regime.

| **Year** | **2018** | | | | | | **2019** | | | | | |
|---|---|---|---|---|---|---|---|---|---|---|---|---|
| Treatment | FN110 | FN165 | CN110 | CN165 | IN110 | IN165 | FN110 | FN165 | CN110 | CN165 | IN110 | IN165 |
| $NPP_{grain}$ (kg C ha$^{-1}$) | 2824 ± 71e | 3578 ± 126cd | 3766 ± 89c | 4765 ± 119a | 3490 ± 106d | 4290 ± 87b | 1928 ± 42g | 2538 ± 53f | 2985 ± 98e | 3580 ± 186cd | 2829 ± 97e | 3573 ± 114cd |
| $NPP_{stem}$ (kg C ha$^{-1}$) | 1529 ± 38e | 1934 ± 59b | 1738 ± 49cd | 2062 ± 61a | 1685 ± 56cd | 2031 ± 46ab | 1285 ± 34f | 1693 ± 58cd | 1687 ± 53cd | 2046 ± 41a | 1648 ± 29d | 1781 ± 46c |
| $NPP_{leaf}$ (kg C ha$^{-1}$) | 514 ± 13g | 664 ± 14cd | 644 ± 20de | 741 ± 19a | 621 ± 21e | 684 ± 16bc | 402 ± 12h | 613 ± 16e | 562 ± 17f | 702 ± 19b | 522 ± 15g | 632 ± 17de |
| $NPP_{root}$ (kg C ha$^{-1}$) | 610 ± 13b | 716 ± 22a | 465 ± 17e | 569 ± 21c | 507 ± 15d | 627 ± 17b | 472 ± 17de | 627 ± 15b | 416 ± 17f | 507 ± 16d | 452 ± 14e | 597 ± 18bc |
| $NPP_{litter}$ (kg C ha$^{-1}$) | 268 ± 6e | 339 ± 10c | 327 ± 8cd | 402 ± 10a | 314 ± 10d | 371 ± 9b | 205 ± 5f | 270 ± 7e | 279 ± 9e | 339 ± 9c | 272 ± 7e | 321 ± 9cd |
| $NPP_{rhizodeposit}$ (kg C ha$^{-1}$) | 602 ± 14e | 758 ± 24c | 727 ± 17cd | 895 ± 22a | 693 ± 22d | 839 ± 18b | 450 ± 11f | 602 ± 15e | 622 ± 20e | 752 ± 27c | 600 ± 16e | 724 ± 20cd |
| *NPP* (kg C ha$^{-1}$) | 6347 ± 148e | 7988 ± 249c | 7666 ± 181cd | 9435 ± 234a | 7310 ± 229d | 8841 ± 190b | 4742 ± 119f | 6343 ± 159e | 6552 ± 213e | 7926 ± 285c | 6323 ± 173e | 7628 ± 211cd |

Statistical analysis

| Year (A) | Irrigation regime (B) | N fertilization (C) | $NPP_{grain}$ (kg C ha$^{-1}$) | $NPP_{stem}$ (kg C ha$^{-1}$) | $NPP_{leaf}$ (kg C ha$^{-1}$) | $NPP_{root}$ (kg C ha$^{-1}$) | $NPP_{litter}$ (kg C ha$^{-1}$) | $NPP_{rhizodeposit}$ (kg C ha$^{-1}$) |
|---|---|---|---|---|---|---|---|---|
| A (year) | | | *** | *** | *** | *** | *** | *** |
| | B (irrigation regime) | | *** | *** | *** | *** | *** | *** |
| | | C (N fertilization) | *** | *** | *** | *** | *** | *** |
| | A × B | | * | ** | ns | ** | ns | ns |
| | A × C | | * | ns | ** | ns | ns | ns |
| | B × C | | ns | ** | *** | ns | ns | ns |
| | A × B × C | | ns | * | ns | ns | ns | ns |

Different lowercase letters indicate significant differences between treatments from 2018 to 2019 ($p < 0.05$). Values are presented as the mean ± standard error of 3 replicates. *, $p < 0.05$; **, $p < 0.01$; ***, $p < 0.001$; ns, non-significant F-values. *NPP*, net primary productivity; $NPP_{grain}$, $NPP_{stem}$, $NPP_{leaf}$, $NPP_{root}$, $NPP_{litter}$, and $NPP_{rhizodeposit}$, net primary productivity of grain, stem, leaf, root, litter, and rhizodeposit.

### *3.3. Carbon Mineralized Losses*

Carbon mineralized loss mainly consisted of *Rh* and $CH_4$ fluxes and was visualized during the rice cropping season (Figure 3). The $CH_4$ fluxes of each treatment sharply increased after the turning green stage, where the highest $CH_4$ fluxes were observed at the late tillering stage. Thereafter, $CH_4$ fluxes dramatically decreased at the drainage stage and reached another peak at the jointing-booting stage. Except for the drainage period, $CH_4$ fluxes under FI were higher than CI and II when the same N fertilization level was applied. Methane fluxes reached up to 55.53 mg m$^{-2}$ h$^{-1}$ in FN165. *Rh* in each treatment increased after the turning green stage, where the highest *Rh* fluxes were observed at the late tillering stage and decreased to a low level at the drainage stage. During rice cropping, *Rh* under CI and II was higher than FI when the same N fertilization level was applied. *Rh* reached 9.13 μmol m$^{-2}$ s$^{-1}$ in CN165. Furthermore, the *Rh* and $CH_4$ fluxes under N165 were higher than N110 under all irrigation regimes.

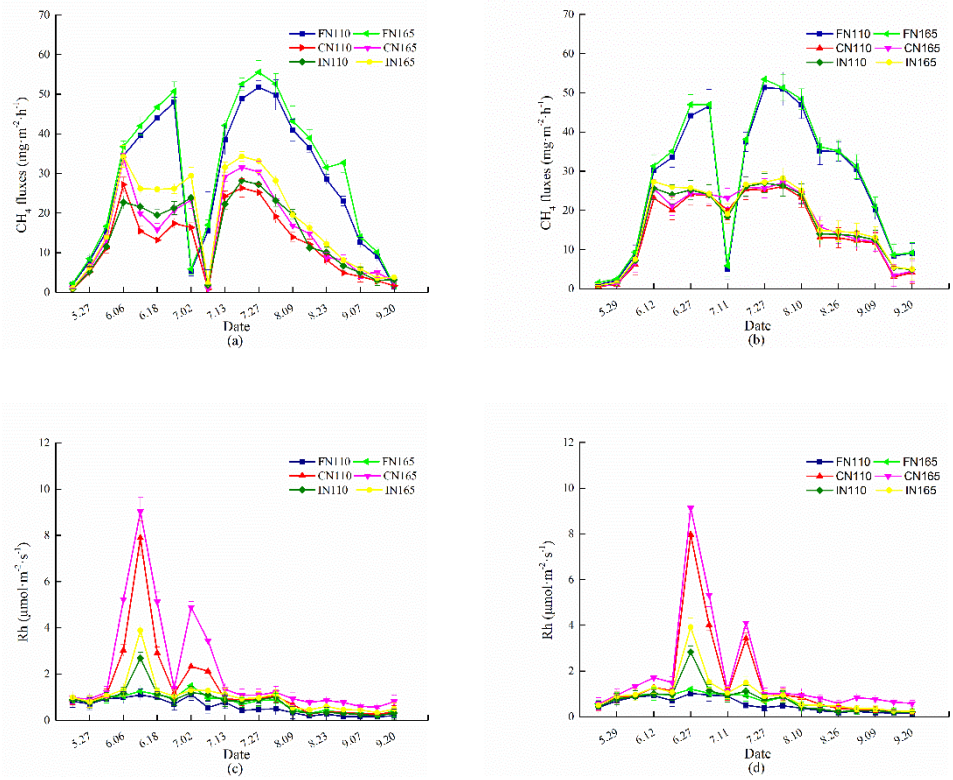


**Figure 3.** Changes in (**a**) CH4 fluxes and (**c**) Rh in 2018 and changes in (**b**) CH4 fluxes and (**d**) Rh in 2019 of paddy field after the implementation of water-saving irrigation.

### *3.4. Net Ecosystem Carbon Budget*

Seasonal *Rh*, $CH_4$ fluxes, and *NECB* are summarized in Table 3. Seasonal *Rh* ranged from 703 to 2709 kg C $ha^{-1}$ at the rice cropping stage. Seasonal *Rh* of CN165 was the highest in 2018, while FN110 was the lowest in 2019. Seasonal *Rh* under CI was significantly higher than FI and II when the same N fertilization level was applied ($p < 0.05$). Seasonal *Rh* under CI was 2.64–3.08 and 1.90–2.19 times higher than FI and II, respectively. Seasonal $CH_4$ fluxes ranged from 389 to 960 kg C $ha^{-1}$ at the rice cropping stage. Seasonal $CH_4$ fluxes of FN165 were the highest, while CN110 was the lowest in 2018. Seasonal $CH_4$ fluxes under FI were significantly higher than CI and II when the same N fertilization level was applied ($p < 0.05$). Seasonal $CH_4$ fluxes under FI were 1.65–2.23 and 1.65–1.70-times higher than CI and II, respectively. Moreover, seasonal *Rh* and $CH_4$ fluxes under N165 were higher than N110 under all irrigation regimes.

**Table 3.** Seasonal *Rh*, $CH_4$ fluxes, *NECB*, and *net GWP* in a paddy field after the implementation of water-saving irrigation.

| Year | Treatment | C Input (kg C $ha^{-1}$) | | C Output (kg C $ha^{-1}$) | | | | *NECB* (kg C $ha^{-1}$) | *net GWP* (kg C $ha^{-1}$) |
|---|---|---|---|---|---|---|---|---|---|
| | | NPP | Sum | Harvest | Rh | $CH_4$ | Sum | | |
| 2018 | FN110 | 6437 ± 148e | 6437 ± 148e | 2824 ± 71e | 758 ± 155ef | 869 ± 20b | 4451 ± 244d | 1896 ± 97c | 17371 ± 252b |
| | FN165 | 7988 ± 249c | 7988 ± 249c | 3578 ± 126cd | 1000 ± 150def | 960 ± 28a | 5538 ± 291c | 2450 ± 76b | 17915 ± 543ab |
| | CN110 | 7666 ± 181cd | 7666 ± 181cd | 3766 ± 89c | 2338 ± 166b | 389 ± 19e | 6493 ± 188b | 1173 ± 8f | 4769 ± 528de |
| | CN165 | 9435 ± 234a | 9435 ± 234a | 4765 ± 119a | 2709 ± 145a | 482 ± 21d | 7956 ± 281a | 1478 ± 123d | 8067 ± 749cd |
| | IN110 | 7310 ± 229d | 7310 ± 229d | 3490 ± 106d | 1067 ± 142de | 516 ± 17cd | 5072 ± 247c | 2238 ± 73b | 6242 ± 246e |
| | IN165 | 8841 ± 190b | 8841 ± 190b | 4290 ± 87b | 1324 ± 143d | 564 ± 19c | 6178 ± 249b | 2663 ± 64a | 6037 ± 416e |

**Table 3.** *Cont.*

| Year | Treatment | C Input (kg C ha$^{-1}$) | | C Output (kg C ha$^{-1}$) | | | | *NECB* (kg C ha$^{-1}$) | *net GWP* (kg C ha$^{-1}$) |
|---|---|---|---|---|---|---|---|---|---|
| | | NPP | Sum | Harvest | Rh | $CH_4$ | Sum | | |
| 2019 | FN110 | 4742 ± 119f | 4742 ± 119f | 1928 ± 42g | 703 ± 140f | 856 ± 40b | 3488 ± 222e | 1255 ± 115ef | 19377 ± 819a |
| | FN165 | 6343 ± 159e | 6343 ± 159e | 2538 ± 53f | 921 ± 164ef | 885 ± 39b | 4344 ± 256d | 1999 ± 112c | 17441 ± 862b |
| | CN110 | 6552 ± 213e | 6552 ± 213e | 2985 ± 98e | 1931 ± 156c | 484 ± 37d | 5401 ± 271c | 1151 ± 134f | 9341 ± 1133c |
| | CN165 | 7926 ± 285c | 7926 ± 285c | 3580 ± 186cd | 2430 ± 156ab | 513 ± 37cd | 6521 ± 378b | 1404 ± 96de | 9196 ± 962c |
| | IN110 | 6323 ± 173e | 6323 ± 173e | 2829 ± 97e | 1008 ± 162def | 513 ± 36cd | 4351 ± 282d | 1973 ± 122c | 7131 ± 801de |
| | IN165 | 7628 ± 211cd | 7628 ± 211cd | 3573 ± 114cd | 1277 ± 153d | 535 ± 37cd | 5386 ± 275c | 2243 ± 113b | 6757 ± 998de |
| Statistical analysis | | | | | | | | | |
| A (year) | | *** | *** | *** | * | ns | *** | *** | ** |
| B (irrigation regime) | | *** | *** | *** | *** | *** | *** | *** | *** |
| C (N fertilization) | | *** | *** | *** | *** | *** | *** | *** | ns |
| A × B | | ns | ns | * | ns | ** | ns | *** | ns |
| A × C | | ns | ns | * | ns | ns | ns | ns | ns |
| B × C | | ns | ns | ns | ns | ns | ns | ** | ns |
| A × B × C | | ns | ns | ns | ns | ns | ns | ns | ns |

Different lowercase letters indicate significant differences between treatments from 2018 to 2019 ($p < 0.05$). Values are presented as the mean ± standard error of 3 replicates. *, $p < 0.05$; **, $p < 0.01$; ***, $p < 0.001$; ns, non-significant F-values. *Rh*, heterotrophic respiration; CH4, seasonal CH4 fluxes; *NPP*, net primary productivity; *NECB*, net ecosystem carbon budget; *net GWP*, net global warming potential.

The *NECB* ranged from 1151 to 2663 kg C ha$^{-1}$, indicating that all treatments acted as a net C sink. The *NECB* of IN165 was the highest in 2018, while CN110 was the lowest in 2019. Results revealed that *NECB* under II was significantly higher than FI and CI when the same N fertilization level was applied ($p < 0.05$). The *NECB* under II was higher than FI and CI by 9–57% and 60–91%, respectively. The *NECB* under FI was higher than CI when the same N fertilization level was applied. The *NECB* under N165 was significantly higher than N110 under all irrigation regimes ($p < 0.05$).

### *3.5. Net Global Warming Potential*

The *net GWP* is summarized in Table 3. The *net GWP* of the *NECB* and $CH_4$ fluxes ranged from 6037 to 19,377 kg C ha$^{-1}$. The *net GWP* of FN110 was the highest in 2019, while IN165 was the lowest in 2018. When the same N fertilization level was applied, *net GWP* under II and CI were significantly lower than FI ($p < 0.05$). The *net GWP* under II was also lower than CI when the N fertilization level was 165 kg N ha$^{-1}$, but no significant differences were detected. Moreover, the *net GWP* under N165 was lower than N110 under II.

## 4. Discussion

Whether paddy field ecosystems function as C sinks or sources is related to the balance of organic C inputs and outputs. It is well-known that appropriate agricultural practice can enhance the ability of C sequestration and mitigate $CO_2$ emissions to combat climate change [50]. In Northeast China, due to the continuous expansion of paddy rice areas, it is imperative to implement water-saving irrigation. Government departments reported that the rice water-saving irrigation area of Heilongjiang Province will exceed $2.8 \times 10^7$ hm$^2$ by 2025, accounting for ~70% of the rice-growing area [51]. However, the status of the C budget in paddy fields remains uncertain. In paddy field ecosystems, Re and C sequestration in rice plants are likely the main processes affecting the C balance. However, additional C inputs (only contain organic fertilizer) and outputs (grain, even straw, except for residues) also affect the C balance of paddy field ecosystems [52,53]. The calculation of *NECB* accounts for all C inputs and outputs to evaluate the C balances of paddy field ecosystems. The *NECB* has been recognized as a scientific evaluation index for determining short-term C balances [54,55].

In single cropping rice paddy ecosystems, more organic C inputs can increase rice dried matter weight, which indicates that SOC stock increases [56,57]. In this study, no additional C inputs were detected, and the C inputs only contained *NPP*. Results revealed that *NPP* under CI and II was higher than FI by 18%–38% and 11%–33%, respectively. This may be because CI and II increased the rice dried matter weight and C contents. These results confirmed that an increase in rice dried matter weight and C contents resulted in increased C inputs. Kim et al. reported that the higher-level N fertilization significantly increased *NPP*, mainly through the increase of rice dried matter weight [39]. These findings were consistent with the results of this study. This study showed that *NPP* under N165 was higher than N110.

In single cropping rice paddy ecosystems, harvest removal (grain, including straw, except for residues) and C mineralized loss are the main C output sources [58,59]. In China, the policy stipulates that anyone who burns straw will be punished, so most farmers return all straw to the field at the time of harvest. In this region, grain was removed at the time of harvest, and harvest removal only contained $NPP_{grain}$. Approximately 55–69% of C outputs were covered by harvest removal, while 30–45% were covered by C mineralized loss. These results indicated that C mineralized loss accounts for a small proportion of C outputs relative to harvest removal; thus, the contribution of C mineralized loss to *NECB* was smaller than $NPP_{grain}$.

*Rh* and $CH_4$ are the main pathways of C mineralized loss from soil to the atmosphere in paddy field ecosystems [60]. Seasonal *Rh* under CI was 2.64–3.08 and 1.90–2.19-times higher than FI and II, respectively. No surface water management of water-saving irrigation resulted in a higher *Rh* in the paddy field. The soil oxygen content increases due to frequent alternate wet and dry conditions. The soil organic matter decomposition was promoted mainly through the increases of the soil oxygen content and the redox potential, and its products provide more substrates for *Rh*. Finally, water-saving irrigation keeps the paddy field in shallow water or no surface water conditions and reduces the distance of $CO_2$ emissions into the atmosphere [18]. In this study, seasonal $CH_4$ fluxes under FI were 1.65–2.23 and 1.65–1.70-times higher than CI and II, respectively. Methane production is mainly derived from anaerobic methane bacteria. FI provides a long-term anaerobic environment that promotes methane production [61]. However, water-saving irrigation improves soil aeration, which greatly reduces $CH_4$ production.

The year, irrigation regime, and N fertilization application level of each factor had a significant effect on *NECB*, as well as the interaction between year and N fertilization application level, and the interaction between irrigation regime and N fertilization application level (Table 3). The *NECB* under N165 was significantly higher than N110 under all irrigation regimes. This indicates that the N fertilization level can promote the C sink capacity of paddy fields. The *NECB* under II was higher than FI by 9–57%. These results indicated that the *NECB* increased after the implementation of II, mainly because the increased *NPP* outweighed the increased harvest removal. However, the *NECB* under FI was higher than CI. This may be because the $NPP_{grain}$ of CI was significantly higher than FI.

The year and irrigation regime of each factor had a significant effect on *net GWP* (Table 3). The *net GWP* decreased significantly after the implementation of water-saving irrigation due to increased C losses, which were far lower than the decreased $CH_4$ fluxes. These results confirmed our hypothesis that water-saving irrigation could decrease *net GWP*. Wu et al. found that *NECB* with a positive value can contribute to mitigating GHG emissions [62]. This is consistent with our results, which showed that *net GWP* under II was lower than FI due to the higher *NECB* under II. However, the *NECB* under CI was lower than FI when the same N fertilization level was applied, but its *net GWP* was lower than FI. This may be because seasonal $CH_4$ fluxes under CI were significantly lower than FI, indicating that $CH_4$ fluxes can also contribute to mitigating GHG emissions. However, the current study had some limitations. For instance, we only evaluated direct GHG emissions. Emissions from irrigation power consumption, agricultural machinery fuel oil consumption, and other farm operations are also crucial for the C budget of

paddy fields ecosystems [63,64]. All correlative GHG emissions should be considered to evaluate the C budget of paddy field ecosystems after the implementation of water-saving irrigation in future studies. At present, the optimal management pattern we obtained was very consistent with the water-saving and emission reduction policies advocated by the government. Our results also provide data support for the government to determine the appropriate irrigation methods and fertilizer amounts. At the same time, the government should strengthen the promotion to enhance farmers' awareness of water-saving irrigation. On the one hand, water-saving irrigation reduces farmers' planting costs; on the other hand, water-saving irrigation reduces the indirect emissions caused by irrigation involved in life cycle assessment (LCA).

## 5. Conclusions

In Northeast China, we conducted a two-year field experiment to measure *Rh*, $CH_4$ fluxes, and *NPP* and calculated *NECB* and *net GWP*. Results showed that single cropping rice paddy fields under each treatment act as net C sinks. The *NECB* was positive and ranged from 1151 to 2663 kg C $ha^{-1}$. Compared to FI, single cropping rice paddy fields enhanced C sink intensity after the implementation of II. II increased the *NECB* through increasing *NPP*, which exceeded the increased removal of harvest and C mineralized losses. The *NECB* under II was higher than that of FI and CI by 9–57% and 60–91%, respectively. Compared to FI, the *net GWP* decreased after the implementation of CI and II. The *net GWP* under II was also lower than CI when the N fertilization level was 165 kg N $ha^{-1}$ in 2018 and 2019. These results indicate that II with 165 kg N $ha^{-1}$ is the optimal management pattern for paddy fields as it can decrease *net GWP* in Northeast China to combat global climate change. Furthermore, the LCA considering indirect GHG emissions should be applied to evaluate the C of paddy field ecosystems after the implementation of water-saving irrigation in future studies.

**Author Contributions:** Methodology, T.L.; software, J.L.; validation, Z.Z. (Zhongxue Zhang) and Z.Q.; formal analysis, T.N. and P.C.; investigation, Y.H. and L.J.; data curation, T.L.; writing—original draft preparation, T.L.; writing—review and editing, Z.Z. (Zhongxue Zhang) and Z.Z. (Zuohe Zhang); funding acquisition, Z.Z. (Zhongxue Zhang). All authors have read and agreed to the published version of the manuscript.

**Funding:** This study was funded by the National Program on Key Basic Research Project of China (2016YFC0400108), General Projects of the National Natural Science Foundation of China (52079028), and the Opening Project of Key Laboratory of Efficient Use of Agricultural Water Resources, Ministry of Agriculture and Rural Affairs of the People's Republic of China in Northeast Agricultural University (AWR2021002).

**Data Availability Statement:** The data presented in this study are available on request from the corresponding author.

**Acknowledgments:** We would like to thank the Heilongjiang Province Hydraulic Research Institute for providing us access to the test sites, as well as for their valuable time providing us with management information. We would also like to acknowledge the National Bureau of Statistics of China for their data support.

**Conflicts of Interest:** The authors declare no conflict of interest.

## References

1. FAO. 2019. Available online: http://www.fao.org/faostat/zh/#data (accessed on 18 March 2020).
2. Dinar, A.; Tieu, A.; Huynh, H. Water scarcity impacts on global food production. *Glob. Food Secur.* **2019**, *23*, 212–226. [CrossRef]
3. Xu, H.; Tian, Z.; He, X.; Wang, J.; Sun, L.; Fischer, G.; Fan, D.; Zhong, H.; Wu, W.; Pope, E.; et al. Future increases in irrigation water requirement challenge the water-food nexus in the northeast farming region of China. *Agric. Water Manag.* **2019**, *213*, 594–604. [CrossRef]
4. Dong, W.; Guo, J.; Xu, L.; Song, Z.; Zhang, J.; Tang, A.; Zhang, X.; Leng, C.; Liu, Y.; Wang, L.; et al. Water regime-nitrogen fertilizer incorporation interaction: Field study on methane and nitrous oxide emissions from a rice agroecosystem in Harbin, China. *J. Environ. Sci.* **2017**, *64*, 289–297. [CrossRef] [PubMed]

5. Towa, J.J.; Guo, X. Effects of irrigation and weed-control methods on growth of weed and rice. *Int. J. Agr. Biol. Eng.* **2014**, *7*, 22–33.
6. Yao, F.; Huang, J.; Cui, K.; Nie, L.; Xiang, J.; Liu, X.; Wu, W.; Chen, M.; Peng, S. Agronomic performance of high-yielding rice variety grown under alternate wetting and drying irrigation. *Field Crop. Res.* **2012**, *126*, 16–22. [CrossRef]
7. Yang, S.; Sun, X.; Ding, J.; Jiang, Z.; Liu, X.; Xu, J. Effect of biochar addition on $CO_2$ exchange in paddy fields under water-saving irrigation in Southeast China. *J. Environ. Manag.* **2020**, *271*, 111029. [CrossRef]
8. Zhuang, Y.; Zhang, L.; Li, S.; Liu, H.; Zhai, L.; Zhou, F.; Ye, Y.; Ruan, S.; Wen, W. Effects and potential of water-saving irrigation for rice production in China. *Agric. Water Manag.* **2019**, *217*, 374–382. [CrossRef]
9. Akter, M.; Deroo, H.; Kamal, A.M.; Kader, M.A.; Verhoeven, E.; Decock, C.; Boeckx, P.; Sleutel, S. Impact of irrigation management on paddy soil N supply and depth distribution of abiotic drivers. *Agric. Ecosyst. Environ.* **2018**, *261*, 12–24. [CrossRef]
10. Wang, M.; Yu, S.; Shao, G.; Gao, S.; Wang, J.; Zhang, Y. Impact of Alternate Drought and Flooding Stress on Water Use, and Nitrogen and Phosphorus Losses in a Paddy Field. *Pol. J. Environ. Stud.* **2018**, *27*, 345–355. [CrossRef]
11. Kögel-Knabner, I.; Amelung, W.; Cao, Z.; Fiedler, S.; Frenzel, P.; Jahn, R.; Kalbitz, K.; Kölbl, A.; Schloter, M. Biogeochemistry of paddy soils. *Geoderma* **2010**, *157*, 1–14. [CrossRef]
12. Li, Z.-G.; Zhang, R.-H.; Wang, X.-J.; Wang, J.-P.; Zhang, C.-P.; Tian, C.-Y. Carbon Dioxide Fluxes and Concentrations in a Cotton Field in Northwestern China: Effects of Plastic Mulching and Drip Irrigation. *Pedosphere* **2011**, *21*, 178–185. [CrossRef]
13. Miyata, A.; Leuning, R.; Denmead, O.T.; Kim, J.; Harazono, Y. Carbon dioxide and methane fluxes from an intermittently flooded paddy field. *Agric. For. Meteorol.* **2000**, *102*, 287–303. [CrossRef]
14. Li, C.; Xiong, Y.; Huang, Q.; Xu, X.; Huang, G. Impact of irrigation and fertilization regimes on greenhouse gas emissions from soil of mulching cultivated maize (*Zea mays* L.) field in the upper reaches of Yellow River, China. *J. Clean. Prod.* **2020**, *259*, 120873. [CrossRef]
15. Trost, B.; Prochnow, A.; Meyer-Aurich, A.; Drastig, K.; Baumecker, M.; Ellmer, F. Effects of irrigation and nitrogen fertilization on the greenhouse gas emissions of a cropping system on a sandy soil in northeast Germany. *Eur. J. Agron.* **2016**, *81*, 117–128. [CrossRef]
16. Qi, L.; Niu, H.-D.; Zhou, P.; Jia, R.-J.; Gao, M. Effects of Biochar on the Net Greenhouse Gas Emissions under Continuous Flooding and Water-Saving Irrigation Conditions in Paddy Soils. *Sustainability* **2018**, *10*, 1403. [CrossRef]
17. Qi, Y.; Guo, S.; Dong, Y.; Peng, Q.; Jia, J.; Cao, C.; Sun, L.; Yan, Z.; He, Y. Advances in Research on the Effects of Irrigation on the Greenhouse Gases Emission and Soil Carbon Sequestration in Agro-ecosystem. *Sci. Agric. Sinica.* **2014**, *47*, 1764–1773.
18. Yang, S.; Liu, X.; Liu, X.; Xu, J. Effect of water management on soil respiration and NEE of paddy fields in Southeast China. *Paddy Water Environ.* **2017**, *15*, 787–796. [CrossRef]
19. Nie, T.; Chen, P.; Zhang, Z.; Qi, Z.; Zhao, J.; Jiang, L.; Lin, Y. Effects of irrigation method and rice straw incorporation on $CH_4$ emissions of paddy fields in Northeast China. *Paddy Water Environ.* **2019**, *18*, 111–120. [CrossRef]
20. Peng, S.; He, Y.; Yang, S.; Xu, J.; Hou, H. Mitigation of methane emissions from paddy fields under controlled irrigation. *Trans. Chin. Soc. Agric. Eng.* **2013**, *29*, 100–107.
21. Wang, M.; Zhang, Z.; Lu, C.; Lin, Y. $CH_4$ and $N_2O$ Emissions from Rice Paddy Field and Their GWPs Research in Different Irrigation Modes in Cold Region. *Int. Soil Water Conse.* **2016**, *23*, 95–100.
22. Xin, F.; Xiao, X.; Dong, J.; Zhang, G.; Zhang, Y.; Wu, X.; Li, X.; Zou, Z.; Ma, J.; Du, G.; et al. Large increases of paddy rice area, gross primary production, and grain production in Northeast China during 2000–2017. *Sci. Total Environ.* **2020**, *711*, 135183. [CrossRef] [PubMed]
23. CHINA WATER. 2019. Available online: http://slt.hlj.gov.cn/contents/9/4645.html (accessed on 23 July 2019).
24. Chen, P.; Nie, T.; Chen, S.; Zhang, Z.; Qi, Z.; Liu, W. Recovery efficiency and loss of 15N-labelled urea in a rice-soil system under water saving irrigation in the Songnen Plain of Northeast China. *Agric. Water Manag.* **2019**, *222*, 139–153. [CrossRef]
25. Wang, M.; Zhang, Z. Optimal water-saving irrigation mode reducing $N_2O$ emission from rice paddy field in cold region and increasing rice yield. *Trans. Chin. Soc. Agric. Eng.* **2015**, *31*, 72–79.
26. Zheng, E.; Yang, H.; Zhang, Z. Influence of different nitrogen forms application on rice photosynthesis: Fluorescence with water-saving irrigation in black soil region of Songnen Plain, Northeast China. *Paddy Water Environ.* **2018**, *16*, 795–804.
27. Chen, P.; Xu, J.; Zhang, Z.; Wang, K.; Li, T.; Wei, Q.; Li, Y. Carbon pathways in aggregates and density fractions in Mollisols under water and straw management: Evidence from 13C natural abundance. *Soil Biol. Biochem.* **2022**, *169*, 108684. [CrossRef]
28. Tang, J.; Zhang, R.; Li, H.; Zhang, J.; Chen, S.; Lu, B. Effect of the Applied Fertilization Method under Full Straw Return on the Growth of Mechanically Transplanted Rice. *Plants* **2020**, *9*, 399. [CrossRef]
29. Yan, F.; Sun, Y.; Xu, H.; Yin, Y.; Wang, H.; Wang, C.; Guo, C.; Yang, Z.; Sun, Y.; Ma, J. Effects of wheat straw mulch application and nitrogen management on rice root growth, dry matter accumulation and rice quality in soils of different fertility. *Paddy Water Environ.* **2018**, *16*, 507–518. [CrossRef]
30. Jiang, Z.; Zhong, Y.; Yang, J.; Wu, Y.; Li, H.; Zheng, L. Effect of nitrogen fertilizer rates on carbon footprint and ecosystem service of carbon sequestration in rice production. *Sci. Total Environ.* **2019**, *670*, 210–217. [CrossRef]
31. Li, C.; Zhang, Z.; Guo, L.; Cai, M.; Cao, C. Emissions of $CH_4$ and $CO_2$ from double rice cropping systems under varying tillage and seeding methods. *Atmos. Environ.* **2013**, *80*, 438–444. [CrossRef]
32. Reeves, S.; Wang, W. Optimum sampling time and frequency for measuring N 2 O emissions from a rain-fed cereal cropping system. *Sci. Total Environ.* **2015**, *530–531*, 219–226. [CrossRef]

33. Zhuang, M.; Zhang, J.; Lam, S.K.; Li, H.; Wang, L. Management practices to improve economic benefit and decrease greenhouse gas intensity in a green onion-winter wheat relay intercropping system in the North China Plain. *J. Clean. Prod.* **2018**, *208*, 709–715. [CrossRef]
34. Xu, Y.; Zhan, M.; Cao, C.; Tian, S.; Ge, J.; Li, S.; Wang, M.; Yuan, G. Improved water management to reduce greenhouse gas emissions in no-till rapeseed–rice rotations in Central China. *Agric. Ecosyst. Environ.* **2016**, *221*, 87–98. [CrossRef]
35. Lou, Y.; Li, Z.; Zhang, T.; Liang, Y. $CO_2$ emissions from subtropical arable soils of China. *Soil Biol. Biochem.* **2004**, *36*, 1835–1842. [CrossRef]
36. Singh, S.; Singh, J.S.; Kashyap, A.K. Methane flux from irrigated rice fields in relation to crop growth and N-fertilization. *Soil Biol. Biochem.* **1999**, *31*, 1219–1228. [CrossRef]
37. Haque, M.M.; Kim, S.Y.; Ali, M.A.; Kim, P.J. Contribution of greenhouse gas emissions during cropping and fallow seasons on total global warming potential in mono-rice paddy soils. *Plant Soil* **2014**, *387*, 251–264. [CrossRef]
38. Ma, Y.C.; Kong, X.W.; Yang, B.; Zhang, X.L.; Yan, X.Y.; Yang, J.C.; Xiong, Z.Q. Net global warming potential and greenhouse gas intensity of annual rice–wheat rotations with integrated soil–crop system management. *Agric. Ecosyst. Environ.* **2013**, *164*, 209–219. [CrossRef]
39. Kim, G.W.; Jeong, S.T.; Kim, P.J.; Gwon, H.S. Influence of nitrogen fertilization on the net ecosystem carbon budget in a temperate mono-rice paddy. *Geoderma* **2017**, *306*, 58–66. [CrossRef]
40. Qi, L.; Pokharel, P.; Chang, S.X.; Zhou, P.; Niu, H.; He, X.; Wang, Z.; Gao, M. Biochar application increased methane emission, soil carbon storage and net ecosystem carbon budget in a 2-year vegetable-rice rotation. *Agr. Ecosyst. Environ.* **2020**, *292*, 106831. [CrossRef]
41. Zeng, W.; Chen, J.; Liu, H.; Wang, W. Soil respiration and its autotrophic and heterotrophic components in response to nitrogen addition among different degraded temperate grasslands. *Soil Biol. Biochem.* **2018**, *124*, 255–265. [CrossRef]
42. Haque, M.M.; Kim, G.W.; Kim, P.J.; Kim, S.Y. Comparison of net global warming potential between continuous flooding and midseason drainage in monsoon region paddy during rice cropping. *Field Crop. Res.* **2016**, *193*, 133–142. [CrossRef]
43. Lun, F.; Liu, Y.; He, L.; Yang, L.; Liu, M.; Li, W. Life cycle research on the carbon budget of the Larix principis-rupprechtii plantation forest ecosystem in North China. *J. Clean. Prod.* **2018**, *177*, 178–186. [CrossRef]
44. Smith, P.; Lanigan, G.; Kutsch, W.L.; Buchmann, N.; Eugster, W.; Aubinet, M.; Ceschia, E.; Béziat, P.; Yeluripati, J.; Osborne, B.; et al. Measurements necessary for assessing the net ecosystem carbon budget of croplands. *Agric. Ecosyst. Environ.* **2010**, *139*, 302–315. [CrossRef]
45. Yan, L.; Zhou, G.S.; Wang, Y.H.; Hu, T.Y.; Sui, X.H. The spatial and temporal dynamics of carbon budget in the alpine grasslands on the Qinghai-Tibetan Plateau using the Terrestrial Ecosystem Model. *J. Clean. Prod.* **2015**, *107*, 195–201. [CrossRef]
46. Kimura, M.; Murase, J.; Lu, Y. Carbon cycling in rice field ecosystems in the context of input, decomposition and translocation of organic materials and the fates of their end products ($CO_2$ and $CH_4$). *Soil Biol. Biochem.* **2004**, *36*, 1399–1416. [CrossRef]
47. Jones, D.L.; Nguyen, C.; Finlay, R.D. Carbon flow in the rhizosphere: Carbon trading at the soil–root interface. *Plant Soil* **2009**, *321*, 5–33. [CrossRef]
48. Hwang, H.Y.; Kim, G.W.; Kim, S.Y.; Haque, M.; Khan, M.I.; Kim, P.J. Effect of cover cropping on the net global warming potential of rice paddy soil. *Geoderma* **2017**, *292*, 49–58. [CrossRef]
49. IPCC. *Climate Change 2013: The Physical Science Basis: Working Group I Contribution to the Fifth Assessment Report of the Intergovernmental Panel on Climate Change*; Cambridge University Press: Cambridge, UK, 2013.
50. Soussana, J.-F.; Tallec, T.; Blanfort, V. Mitigating the greenhouse gas balance of ruminant production systems through carbon sequestration in grasslands. *Animal* **2010**, *4*, 334–350. [CrossRef]
51. HLJNEWS. 2019. Available online: http://slt.hlj.gov.cn/contents/9/4001.html (accessed on 1 January 2019).
52. Mudge, P.L.; Wallace, D.F.; Rutledge, S.; Campbell, D.I.; Schipper, L.A.; Hosking, C.L. Carbon balance of an intensively grazed temperate pasture in two climatically contrasting years. *Agric. Ecosyst. Environ.* **2011**, *144*, 271–280. [CrossRef]
53. Zeeman, M.J.; Hiller, R.; Gilgen, A.K.; Michna, P.; Plüss, P.; Buchmann, N.; Eugster, W. Management and climate impacts on net $CO_2$ fluxes and carbon budgets of three grasslands along an elevational gradient in Switzerland. *Agric. For. Meteorol.* **2010**, *150*, 519–530. [CrossRef]
54. Byrne, K.A.; Kiely, G.; Leahy, P. Carbon sequestration determined using farm scale carbon balance and eddy covariance. *Agric. Ecosyst. Environ.* **2007**, *121*, 357–364. [CrossRef]
55. Song, C.; Wang, G.; Hu, Z.; Zhang, T.; Huang, K.; Chen, X.; Li, Y. Net ecosystem carbon budget of a grassland ecosystem in central Qinghai-Tibet Plateau: Integrating terrestrial and aquatic carbon fluxes at catchment scale. *Agric. For. Meteorol.* **2020**, *290*, 108021. [CrossRef]
56. Pan, G.X.; Li, L.Q.; Wu, L.S.; Zhang, X.H. Storage and sequestration potential of topsoil organic carbon in China's paddy soils. *Glob. Change Biol.* **2004**, *10*, 79–92. [CrossRef]
57. Zhao, X.; Wang, J.; Wang, S.; Xing, G. Successive straw biochar application as a strategy to sequester carbon and improve fertility: A pot experiment with two rice/wheat rotations in paddy soil. *Plant Soil* **2014**, *378*, 279–294. [CrossRef]
58. Jia, J.X.; Ma, Y.C.; Xiong, Z.Q. Net ecosystem carbon budget, net global warming potential and greenhouse gas intensity in intensive vegetable ecosystems in China. *Agric. Ecosyst. Environ.* **2012**, *150*, 27–37. [CrossRef]
59. Yadav, G.S.; Das, A.; Lal, R.; Babu, S.; Meena, R.S.; Saha, P.; Singh, R.; Datta, M. Energy budget and carbon footprint in a no-till and mulch based rice–mustard cropping system. *J. Clean. Prod.* **2018**, *191*, 144–157. [CrossRef]

60. Janzen, H.H. Carbon cycling in earth systems—A soil science perspective. *Agric. Ecosyst. Environ.* **2004**, *104*, 399–417. [CrossRef]
61. Shakoor, A.; Gan, M.Q.; Yin, H.X.; Yang, W.; He, F.; Zuo, H.F.; Ma, Y.H.; Yang, S.Y. Influence of nitrogen fertilizer and straw returning on $CH_4$ emission from a paddy field in chao lake basin, China. *Appl. Ecol. Environ. Res.* **2020**, *18*, 1585–1600. [CrossRef]
62. Wu, L.; Wu, X.; Lin, S.; Wu, Y.; Tang, S.; Zhou, M.; Shaaban, M.; Zhao, J.; Hu, R.; Kuzyakov, Y.; et al. Carbon budget and greenhouse gas balance during the initial years after rice paddy conversion to vegetable cultivation. *Sci. Total Environ.* **2018**, *627*, 46–56. [CrossRef]
63. Xia, L.; Ti, C.; Li, B.; Xia, Y.; Yan, X. Greenhouse gas emissions and reactive nitrogen releases during the life-cycles of staple food production in China and their mitigation potential. *Sci. Total Environ.* **2016**, *556*, 116–125. [CrossRef]
64. Zhang, M.; Li, B.; Xiong, Z.Q. Effects of organic fertilizer on net global warming potential under an intensively managed vegetable field in southeastern China: A three-year field study. *Atmos. Environ.* **2016**, *145*, 92–103. [CrossRef]